Scientific Paper / Artículo Científico

INGENIUS
Revista de Ciencia y Tecnología
https://doi.org/10.17163/ings.n29.2023.01
pISSN: 1390-650X / eISSN: 1390-860X

Voltage stability and electronic compensation in electrical power systems using simulation models

Estabilidad de tensión y compensación electrónica en sistemas eléctricos de potencia usando herramientas de simulación

M. Campaña[1,*], P. Masache[1], E. Inga[1], D. Carrión[1]

Received: 21-04-2021, Received after review: 24-09-2021, Accepted: 08-11-2021, Published: 01-01-2023

Abstract

Increased demand in the different electrical power systems (EPS) has a negative impact in voltage stability, reliability and quality of the power supply. Voltage profile is reduced when generation units are not capable of supplying reactive power to the EPS at the times it is required. With the development of power electronics and complex control systems, flexible alternating current transmission system (FACTS) devices have been introduced. In this article, the impact of the introduction of a type of FACTS that allows reactive power compensation in the EPS is analyzed in detail. Furthermore, a methodology to decide the capacity of the Static Synchronous Compensator (STATCOM) and its optimal location with the execution of continuous power flows (CPF) will be analyzed. Finally, the positive impact of installing a Power System Stabilizer (PSS) control to ensure voltage stability in the EPS will be studied. This article is developed using the IEEE 14-bus base system under two mathematical models for power flow calculation developed in MATLAB software, which are: which are: i) through the power balance equations and ii) Newton Raphson with the toolbox PSAT.

Keywords: Load Factor, PSAT, contingency, Continuous Power Flow, PSS, STATCOM

Resumen

El aumento de la demanda en los distintos sistemas eléctricos de potencia (SEP) tiene un impacto negativo en la estabilidad de la tensión, la confiabilidad y la calidad del suministro eléctrico. El perfil de tensión disminuye cuando las unidades de generación no son capaces de suministrar potencia reactiva al sistema eléctrico en los momentos que se requiere. Con el desarrollo de la electrónica de potencia y los complejos sistemas de control, se han podido introducir dispositivos de sistemas flexibles de transmisión de corriente alterna (FACTS, del inglés *Flexible Alternating Current Transmission System*). En este artículo se analiza en detalle el impacto que genera la introducción de un tipo de FACTS que permite la compensación de potencia reactiva en el SEP. Además, se analizará una metodología para decidir la capacidad del compensador síncrono estático (STATCOM, del inglés *Static Synchronous Compensator*) y su ubicación óptima con la ejecución de flujos de potencia continuos (FPC). Finalmente, se estudiará el impacto positivo de la instalación de un control estabilizador de potencia (PSS, del inglés *Power System Stabilizer*) para asegurar la estabilidad de tensión en el SEP. Este artículo se desarrolla utilizando el sistema base IEEE de 14 barras bajo dos modelos matemáticos para el cálculo del flujo de potencia desarrollados en el software Matlab, que son: i) utilizando las ecuaciones de balance de potencia y ii) Newton Raphson con el *toolbox* de MATLAB (PSAT, del inglés *Power System Analysis Toolbox*).

Palabras clave: factor de carga, PSAT, contingencia, flujo de potencia continuo, PSS, STATCOM

[1,*]Grupo de Investigación de Redes eléctricas Inteligentes (GIREI), Universidad Politécnica Salesiana - Ecuador.
Corresponding author ✉: mcampana@ups.edu.ec.

Suggested citation: Campaña, M.; Masache, P.; Inga, E. and Carrión, D. "Voltage stability and electronic compensation in electrical power systems using simulation models," *Ingenius, Revista de Ciencia y Tecnología*, N.° 29, pp. 9-23, 2023, DOI: https://doi.org/10.17163/ings.n29.2023.01.

1. Introducción

Most interruptions in electric transmission networks (ETN) are due to voltage instability. Possible causes may be overloaded electric systems, occurrence of faults or lack of available reactive power in generation units. At present, it is possible to have a greater control of the voltage margin on each of the buses of the EPS [1–3]. The ETN are responsible for supplying electric power from the generation units to the loads, meeting safety and reliability criteria. The shortage of reactive power that a generation unit may supply to the system may be due to a load increase in the EPS, causing a possible degradation of the voltage stability in the electric system [4, 5], especially in buses that operate close to their limits. It is shown in [6] that the maximum capacity for transferring electric power through the ETN may be improved installing FACTS devices. Such devices may anticipate control of power flow and voltage profile, improve voltage stability and minimize losses. However, their high cost limits the installation of FACTS controllers in all lines of the EPS. It is assured in [7, 8] that the best FACTS devices are those based on converters such as: STATCOM and the Unified Power Flow Controller (UPFC). The present paper will pay special attention to the synchronous static compensator and its direct control on voltage stability.

Another detail addressed in this paper is the dynamic analysis in the presence of electromechanical oscillations in the EPS. These oscillations may be local (a single generator) or may involve a number of generators widely separated geographically (oscillations between areas). If they are not controlled, these oscillations may lead to a partial or total interruption of the power supply [9]. Electromechanical oscillations may be damped through the application of PSS. The objective of the PSS is to modulate the extinction voltage of a synchronous generator acting through the automatic voltage regulator (AVR) [10, 11], and are economically viable for improving voltage stability in the presence of small disturbances [12–14]. Therefore, PSS use auxiliary stabilizing signals, such as shaft speed, terminal frequency and power to vary the AVR input signal. The block diagram of the PSS used in this paper may be verified in [9], [15, 16]. Regarding this aspect, one of the main contributions of this paper is proving that the voltage instability produced by an $N-1$ contingency (opening of a line) may be eliminated adding a PSS in bus 1 of the proposed EPS (Figure 1).

The objective of this paper is to study voltage stability and the direct effects of installing synchronous static compensators in buses whose nominal voltage is critical, i.e., it is below or about to go below the lower voltage limit (0.95 pu). The IEEE 14-bus system is used as a base case to validate the proposed methodology. In addition, through the application of PSS and simulations in time-domain with the PSAT toolbox, it will be proven that power stabilizing systems may enable maintaining EPS stability or reducing the negative effect on it of an $N-1$ contingency. To achieve the objective of this paper, power flows will be simulated in static state under two iterative mathematical models based on power balance equations and Newton Raphson methodology. In addition, this analysis will enable evaluating the performance and error margins between each model. It is very important to mention that the Matlab software and the PSAT toolbox developed by Federico Milano will be used here.

The power flow analysis will help to verify the steady state magnitude of voltage, angle and active and reactive power of both load and generation. The different operating states will vary according to various initial parameters set on the EPS obtained from the IEEE 14-bus base case. These parameters will enable generating unstable conditions in the EPS, and further evaluating and being able to determine the best technical action to recover stability in the electric power system. The actions to which the system will be subject are: i) symmetrical increase of the load by a load factor λ that will directly multiply the active and reactive power of all loads and ii) opening of lines that simulate $N-1$ contingencies.

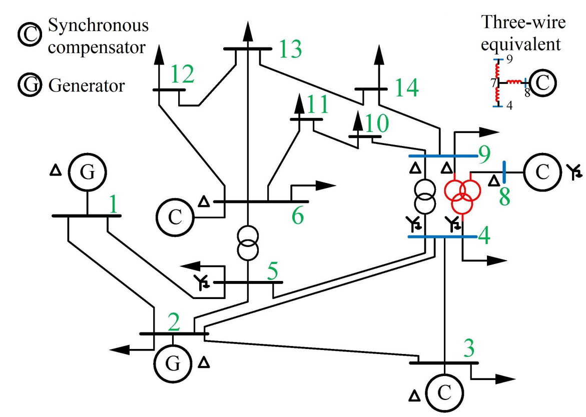

Figure 1. IEEE 14-bus system base case

Section II briefly analyzes the positive impact on the voltage profiles of an EPS when using synchronous static compensation in power transfer buses. Section III formulates the problem and explains the methodology applied in this paper. Section IV presents the results obtained in the simulations. At last, conclusions are presented in section V.

2. Materials y methods

The FACTS devices are not only capable of controlling the power transmitted and increasing the capacity of the lines, but also may suppress power fluctuations [4], [17, 18]. These devices are constructed with static elements and power electronics elements which, together, enable improving control and increasing the energy transfer capacity in alternating current (AC) systems. The operating principle of the synchronous compensator, which is a type of FACTS, considers three fundamental criteria i) a direct current (DC) capacitor after a transformer operates as a controllable voltage source, (ii) the voltage difference at the transformer reactance produces exchanges of active and reactive power between the STATCOM and the SEP and iii) the magnitude of the STATCOM output voltage may be controlled varying the voltage across the CC capacitor [19–21]. Figure 2 illustrates a basic structure that summarizes the STATCOM architecture.

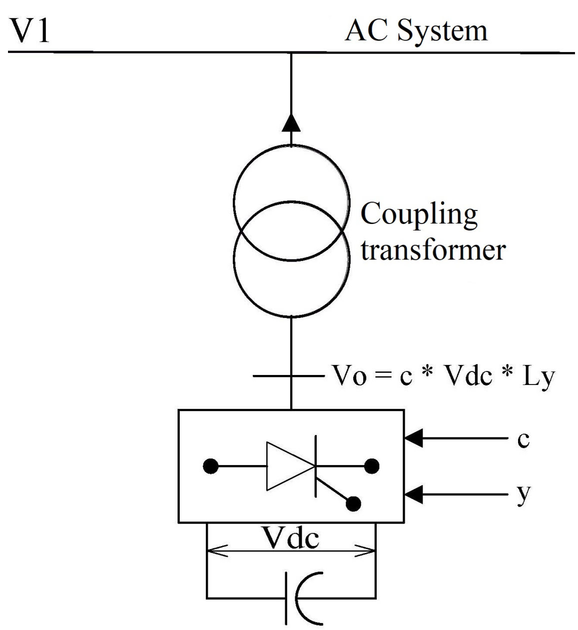

Figure 2. Basic structure of a type 2 STATCOM

There are two types of synchronous static compensators: the type 1 compensator is able to control active and reactive power in a transmission line, while type 2 can only control the angle ψ and the gain c remains fixed. ψ is the angular difference between V_1 (voltage at the STATCOM bus) and V_0 (Figure 2). In addition, the value of ψ should be kept very small to be able to control the system reactive power and desired voltage. For small values of ψ, the reactive power supplied by the STATCOM has a linear relationship [22,23]. Therefore, type 2 static synchronous compensators are not able to supply active power, because they spend active power to compensate transformer and commutation losses. Consequently, according to the voltage level of the system and the type of compensator, the STATCOM may operate as a capacitor or as an inductor. It is important to mention that the type 2 STATCOM will be used in this paper. The STATCOM may be modeled as a synchronous voltage source with maximum and minimum limits of voltage magnitude. In addition, the STATCOM obeys limits and according to the requirements is capable of generating or absorbing reactive power [24–26]. It is important to mention that in this paper the STATCOM will be modeled as a voltage source enabling a rigid voltage support mechanism.

The methodology implemented to analyze the problem considers the following statements: i) an analysis of the power flow in the system from differential equations comparing it with the Newton Raphson method and ii) stability analysis of angle and voltage. The EPS analyzed in this paper is illustrated in Figure 1. The system has 5 generation buses, 11 loads and 20 transmission lines. The base of the system is 100 MVA and bus 1 is defined as Slack or reference bus. The present paper will be analyzed at two moments i) power flow and arbitrary installation of a STATCOM at buses 13 and 14 and ii) it will be analyzed the voltage stability observing CPFs, which will enable to analyze the EPS behavior through the load factor increase. The power flow will be analyzed in two ways i) a mathematical model developed in Matlab considering the power balance equations and ii) the power flow using the PSAT toolbox. This will enable evidencing the error margins and performance of each model.

It is known that a load increase both in active and reactive powers will stress the system, and the reference values of voltage in each bus will be degraded. It the generation units are not capable of supplying the reactive power demanded by the system, these voltage values will decrease. This voltage reduction in the buses will compromise the EPS voltage stability. In the present paper the load factor λ will be increased 50%, i.e., λ will be equal to 1.5 pu. This will stress the system and through a static state power flow it will be possible to observe the voltage magnitudes updated with the load increase. Once the system has been stressed due to the load factor, buses 13 and 14 are chosen (Figure 1) as candidate sites for installing the STATCOM. The fundamental objective is to determine the type of STATCOM and the best location considering technical criteria at the lowest cost. The basic criteria for dimensioning and selecting the best location to install a STATCOM are defined in the literature considering three very important factors, namely: i) it should be chosen the STATCOM with minimum Mvar capacity that ii) guarantees that voltage remains within allowable limits (1.05-0.95 pu) verifying that iii) total reactive power losses in the EPS are minimum. At a second moment, it will be analyzed the stability of the electric system in the presence of $N-1$ contingencies in line 2-4 of Figure 1. Finally, it will be simulated the effect of the STATCOM on the EPS before and after its installation.

A modern electric system consists of a large mixture of renewable energy sources, variable and flexible loads, and is also experiencing a situation in which a significant number of conventional generators are being replaced by sources based on power electronics [27]. Consequently, the EPS stabilizers are controllers installed in synchronous generators whose main function is to dampen the oscillations of the electric system controlling the excitation, with the purpose of increasing the stability margin in the presence of low frequency oscillations in the EPS. The PSS controllers have two structures constituted by i) gain and phase compensation stages and ii) three bands corresponding to a specific frequency range (low, intermediate and high frequency) in which each band is constituted by two branches based on differential filters (with a gain, delay blocks and a hybrid block) [28]. Consequently, the design of power system stabilizers is a challenging task that requires long time, and thus an alternative for controller adjustment is the use of optimization methods [29]. An optimal design of a multimachine PSS is proposed in [30] for various simultaneous steady-state operating conditions.

2.1. Methodology for Power Flow Calculation

To know the behavior of the EPS at an operating point where the power flow is computed; the methodology and equations that model the power flow are detailed below:

- Initialize the unknown variables of the system. Voltage equal to 1 pu and angles equal to 0 rad.
- Admittance of the system (Ybus)

$$Y_{ii} = \sum_{k=1}(\frac{1}{Z_{ik}}) + \sum(Y_i) \tag{1}$$

$$Y_{ij} = -\frac{1}{Z_{ij}} \tag{2}$$

- Equations that govern the power flow

$$P_i = \sum_{k=1}(V_i*V_k*(G_{ik}*cos(\delta_i-\delta_k)+B_{ik}*sin(\delta_i-\delta_k))) \tag{3}$$

$$Q_i = \sum_{k=1}(V_i*V_k*(G_{ik}*sin(\delta_i-\delta_k)-B_{ik}*cos(\delta_i-\delta_k))) \tag{4}$$

- Balance of active and reactive power

$$\Delta P_i = P_{gen_i} - P_{d_i} - P_i \tag{5}$$

$$\Delta Q_i = Q_{gen_i} - Q_{d_i} - Q_i \tag{6}$$

- Jacobian matrix

$$\begin{bmatrix} \frac{d(\Delta P_i)}{d(\delta_i)} & \frac{d(\Delta P_i)}{d(V_i)} * |V_i| \\ \frac{d(\Delta Q_i)}{d(\delta_i)} & \frac{d(\Delta Q_i)}{d(V_i)} * |V_i| \end{bmatrix} = J \tag{7}$$

- Solution of equations

$$\begin{bmatrix} \Delta\delta_i \\ \Delta V_i \end{bmatrix} = J^{-1} * \begin{bmatrix} \Delta P_i \\ \Delta Q_i \end{bmatrix} \tag{8}$$

- New iteration values

$$\begin{bmatrix} \delta_{i+1} \\ V_{i+1} \end{bmatrix} = \begin{bmatrix} \Delta\delta_i \\ \Delta V_i \end{bmatrix} + \begin{bmatrix} \delta_i \\ V_i \end{bmatrix} \tag{9}$$

- Stopping criterion

$$\max\left(\begin{vmatrix} \Delta P_{i+1} \\ \Delta Q_{i+1} \end{vmatrix}\right) \leq 1e^{-5} \tag{10}$$

2.2. System transfer capacity

It enables knowing the maximum power transfer allowed in the electric system when an $N-1$ contingency occurs; the mathematical model given by equations **??**-**??** is used to calculate this index.

- Total transfer capacity

$$TTC = \sum(P_{Load} + \lambda_{max} * \sum(\Delta P_{Loss})) \tag{11}$$

- Real power transmitted

$$ETC = \sum(P_{Load}) \tag{12}$$

- Transmission margin before reaching instability

$$TRM = 0.05 * TTC \tag{13}$$

- Transfer capacity

$$ATC = TTC - ETC - TRM \tag{14}$$

2.3. Voltage stability

Voltage stability may be verified from CPF usage. The objective of CPF is periodically increasing λ to reach the maximum inflection point (λ_{max}) where the stability of the electric system operates at the limit; i.e., when it reaches its maximum value ($\lambda = P_{L_{max}}$), the voltage magnitudes at the different buses of the EPS will decrease until reaching a voltage collapse. The voltage stability analysis is carried out from the power *vs.* voltage curve (PV curves). The PV curve is simulated from the power flow using equations (1)-(10).

3. Results and discussion

This section presents a detailed description of the power flow and voltage stability analysis results. The magnitudes of voltage, angle, active and reactive power of both load and generation are obtained analyzing the EPS at an operating point under specific initial conditions. The EPS topology and its electric parameters (transmission lines and buses) are detailed in Tables 1 and 2 [31]. Table 1 describes the EPS topology and the line impedance parameters. Table 2 details the active and reactive powers of generation, load and base voltage, and also defines the type of line according to the following nomenclature i) 1 Slack bus ii) 2 PV bus and iii) 3 PQ bus.

Table 1. Data of lines in the IEEE 14-bus base case

Line	Line from	Line to	Line impedance [pu] Resistance	Reactance	Bsh/2
01	01	05	0.05403	0.22304	0.0219
02	01	02	0.01938	0.05917	0.0264
03	02	05	0.05695	0.17388	0.0170
04	02	04	0.05811	0.17632	0.0246
05	02	03	0.04699	0.19797	0.0187
06	03	04	0.06701	0.17103	0.0173
07	04	09	0.00000	0.55618	0.0000
08	05	04	0.01335	0.04211	0.0064
09	05	06	0.00000	0.25202	0.0000
10	06	12	0.12291	0.25581	0.0000
11	06	13	0.06615	0.13027	0.0000
12	06	11	0.09498	0.19890	0.0000
13	07	09	0.00000	0.11001	0.0000
14	07	04	0.00000	0.20912	0.0000
15	07	08	0.00000	0.17615	0.0000
16	09	14	0.12711	0.27038	0.0000
17	09	10	0.03181	0.08450	0.0000
18	10	11	0.08205	0.19207	0.0000
19	12	13	0.22092	0.19988	0.0000
20	14	13	0.17093	0.34802	0.0000

Table 2. Data for each Bus in the IEEE 14-bus base case

Bus N.°	Bus Type	P_g [pu]	Q_g [pu]	P_d [pu]	Q_d [pu]	V_m [pu]	Base [kV]
01	1	1.1417	-0.169	0.0000	0.0000	1.060	69.0
02	2	0.4000	0.0000	0.2170	0.1270	1.045	69.0
03	2	0.0000	0.0000	0.9420	0.1910	1.010	69.0
04	3	0.0000	0.0000	0.4780	0.0400	1.000	69.0
05	3	0.0000	0.0000	0.0760	0.0160	1.000	13.8
06	2	0.0000	0.0000	0.1120	0.0750	1.000	13.8
07	3	0.0000	0.0000	0.0000	0.0000	1.000	18.0
08	2	0.0000	0.0000	0.0000	0.0000	1.000	13.8
09	3	0.0000	0.0000	0.2950	0.1660	1.000	13.8
10	3	0.0000	0.0000	0.0900	0.0580	1.000	13.8
11	3	0.0000	0.0000	0.0350	0.0180	1.000	13.8
12	3	0.0000	0.0000	0.0610	0.0160	1.000	13.8
13	3	0.0000	0.0000	0.1380	0.0580	1.000	13.8
14	3	0.0000	0.0000	0.1490	0.0500	1.000	13.8

Once the initial parameters and the features of the ETN have been defined, it is verified the performance of two mathematical models developed in Matlab for power flows. The first model provides an iterative solution based on power balance equations (traditional method), whereas the second model uses the Newton Raphson algorithm with the PSAT toolbox.

3.1. Power flow using computational tools

Figure 3 enables to verify the voltage and angle variation ranges obtained from the simulation. Figure 3(a) shows the node voltage levels at each bus of the EPS for two computation models. The results of the mathematical model proposed in the PSAT toolbox are shown in orange, whereas the solution of the mathematical model proposed in Matlab using power balance equations is shown in blue. In buses 4, 5, 7, 9, 10, 11 and 14 the average error is 0.0037 p.u (Figure 3(a)); it can be seen that the error margin between the two models (Matlab – PSAT) is minimum, technically zero. Figure 3(b) represents the magnitude of the angles in each of the buses of the EPS; similarly, the average error margin in the angle results is 0.0042 radians. Therefore, the two models proposed for analyzing the power flow at steady state provide reliable solutions with minimum error margins. An additional detail that may be seen in Figure 3 is that the voltage magnitudes do not exceed the upper and lower limits of 1.05 pu and 0.95 pu, respectively, except for the Slack bus whose voltage is defined as 1.06 pu due to its nature.

The error margin in the active and reactive power is presented in Figure 4. The average error margin in the active power is 0.0019 pu, as it can be seen in Figure 4(a), whereas the average error margin in the reactive power is 0.0593 pu. A detail that should be taken into account is that both active and reactive power show similar trends, with error margins that approach zero. Therefore, considering only the comparative analysis of the results obtained for both models, presented in Figures 3 and 4, it may be concluded that both ways to obtain a solution to the power flow are reliable. However, Table 3 analyzes the performance of the methods proposed for power flow calculation.

It may be seen in Table 3 that the models execute the same number of iterations; however, the average margin of total active and reactive power losses is 0.0006 and 0.0485, respectively, and thus, it may be concluded that they are minimum and approach zero. It is important to mention that the same value of 1×10^{-5} for the error margin was considered for both methods. On the other hand, the CPU - Time achieved by the conventional method (power flow solved using power balance equations) is approximately 65 time larger (Table 3); hence, the PSAT toolbox is definitely a tool of very good performance, capable of providing reliable solutions in significantly small machine times.

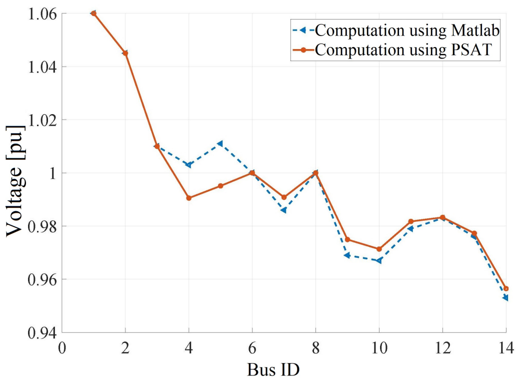

(a) Node voltage in pu

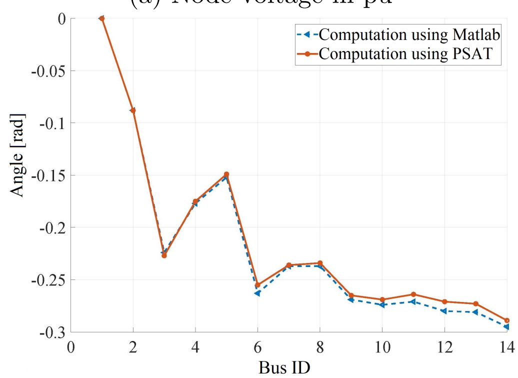

(b) Node angle in radians

Figure 3. Node Analysis of the IEEE 14-bus EPS

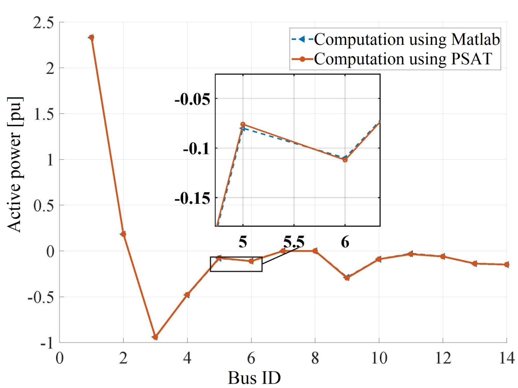

(a) Node active power in pu

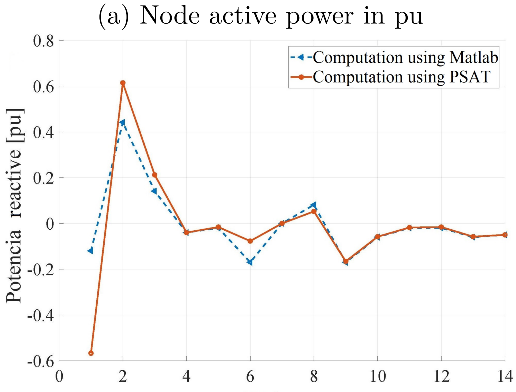

(b) Node reactive power in pu

Figure 4. Node Analysis of the IEEE 14-bus EPS

Table 3. Performance of the mathematical models proposed for computing the power flow

Parameter	Conventional method	Toolbox PSAT
CPU - Time [s]	19.641	0.3020
# of Iterations	4.0000	4.0000
Error margin of total P losses [pu]	0.1440	0.1434
Error margin of total Q losses [pu]	0.2740	0.3225

Table 4 presents the initial results obtained for the power flow, which will be referential magnitudes to start the study of voltage stability. It is very important to mention that the results achieved were extracted from the power flow solution provided by the PSAT Toolbox. As it can be seen, it is possible to monitor the magnitudes of voltage, angle, active and reactive power in each of the EPS buses; all the parameters presented in Table 4 were simulated without constraints in the maximum and minimum limits of active and reactive power.

Therefore, according to the initial values, the electric system operates at normal conditions, which indicates that it honors the voltage limits established by the regulation. In addition, Table 4 shows the total active and reactive power losses in the EPS.

Table 4. Low Newton-Raphson power flow solution in IEEE 14-bus base case

Bus N.°	Voltage [pu]	Angle [rad.]	Generación		Load	
			MW	Mvar	MW	Mvar
01	1.060	0.000	233.0	-5.70	0.000	0.000
02	1.045	-0.088	40.00	74.10	21.70	12.70
03	1.010	-0.227	0.000	40.30	94.20	19.10
04	0.991	-0.175	0.000	0.000	47.80	4.000
05	0.995	-0.149	0.000	0.000	7.600	1.600
06	1.000	-0.255	0.000	-0.200	11.20	7.500
07	0.991	-0.236	0.000	0.000	0.000	0.000
08	1.000	-0.234	0.000	5.200	0.000	0.000
09	0.975	-0.265	0.000	0.000	29.50	16.60
10	0.971	-0.269	0.000	0.000	9.000	5.800
11	0.982	-0.264	0.000	0.000	3.500	1.800
12	0.983	-0.271	0.000	0.000	6.100	1.600
13	0.977	-0.273	0.000	0.000	13.50	5.800
14	0.956	-0.289	0.000	0.000	14.90	5.000
Suma			273.6	113.8	259.3	81.50
Total power loss						
Active [MW]	14.34					
Reactive [Mvar]	32.25					

Table 55 presents the results for a load factor of 50% both in active and reactive power. In addition, the power flow is constrained to obey the power limits on the generation buses whose magnitudes oscillate between 0.5 p.u. for the active power and -0.06 p.u. for the reactive power. If the two cases presented in Tables 4 and 5 are compared, it may be seen the increase in active and reactive power, both generated and consumed. However, the voltage magnitudes in bus 14 fell below the lower limit of 0.95 pu (Table 5).

Table 5. Power flow solution for 50% load increase conditions with respect to the IEEE 14-bus base case

Bus N.°	Voltage [pu]	Angle [rad.]	Generation		Load	
			MW	Mvar	MW	Mvar
01	1.070	0.000	384.4	0.000	0.000	0.000
02	1.045	-0.145	40.00	114.2	32.60	19.10
03	1.010	-0.361	0.000	81.40	141.3	28.70
04	0.973	-0.281	0.000	0.000	71.70	6.000
05	0.980	-0.239	0.000	0.000	11.40	2.400
06	1.000	-0.405	0.000	26.90	16.80	11.30
07	0.973	-0.370	0.000	0.000	0.000	0.000
08	1.000	-0.370	0.000	15.20	0.000	0.000
09	0.948	-0.419	0.000	0.000	44.30	24.90
10	0.945	-0.425	0.000	0.000	13.50	8.700
11	0.966	-0.419	0.000	0.000	5.300	2.700
12	0.973	-0.431	0.000	0.000	9.200	2.400
13	0.963	-0.433	0.000	0.000	20.70	8.700
14	0.924	-0.457	0.000	0.000	22.40	7.500
Suma			424.4	237.0	389.0	122.3
		Total power loss				
Active [MW]		35.46				
Reactive [Mvar]		115.5				

The new power flow, considering active power limits with the implementation of STATCOM in buses 13 and 14, is illustrated in Table 6. It is very important to remember that the STATCOM is modeled as a voltage source. The initial parameters of the voltage source are fixed at 1 pu and 0 degrees, and thus, when a power flow is executed with the PSAT Toolbox it will be obtained the reactive power necessary to compensate and maintain the required voltage magnitude at 1 p.u. in the STATCOM installation bus. In other words, this magnitude of generated reactive power will be necessary to compensate the system for a load factor increase of $\lambda = 1.5$ pu of the demand. As it can be seen in Table 6, the generation reactive power to maintain the voltage in buses 13 and 14 at 1 pu at different instants, reaches magnitudes of 40.5 and 34.8 Mvar respectively. In addition, it should be noted that when the STATCOM is placed at bus 13 the voltage profiles do not reach the admissible minimum values, whereas when it is placed at bus 14 the bus voltages have appropriate values. An additional detail is that the EPS at normal and stress conditions ($\lambda = 1.5$ pu) records minimum magnitudes of 0.956 and 0.924, respectively, in bus 14, which implies this is a candidate bus to install the STATCOM because it exhibits lower voltage magnitudes in pu; therefore, it requires to be compensated with reactive power to raise the voltage magnitude to appropriate ranges.

On the other hand, Table 6 presents total active and reactive power losses. It may be seen that the active power loss is of equal magnitude, regardless of the bus where the STATCOM is installed. However, there is a slight difference in terms of the total reactive power loss if the STATCOM is installed in buses 13 or 14 (Table 6), with the smaller magnitude corresponding to the case when the STATCOM is installed in bus 14. Therefore, when minimizing total losses of reactive power, the optimal location of the STATCOM is determined by the requirement of maintaining the voltage profiles in moderate ranges and being the one with the lowest class. Class refers to the magnitude of Mvar required for the STATCOM. Finally, when the load factor is increased in 50% in all PQ buses (load buses), it is required to install a STATCOM of class 34.80 Mvar in bus 14 with the purpose of maintaining the voltage levels at allowable magnitudes, thus guaranteeing voltage stability using synchronous static compensation to minimize losses. When losses are minimized, the power flow transfer capacity is maximized in the EPS, as specified in the literature.

Table 6. Power flow solution applying STATCOM to the IEEE 14-bus base case

Bus N.°	STATCOM Barra 13						STATCOM Barra 14					
	Voltage [pu]	Angle [rad.]	Generation MW	Generation Mvar	Load MW	Load Mvar	Voltage [pu]	Angle [rad.]	Generation MW	Generation Mvar	Load MW	Load Mvar
01	1.070	0.000	384.5	0.000	0.000	0.000	1.071	0.000	384.3	0.000	0.000	0.000
02	1.045	-0.145	40.00	113.0	32.60	19.10	1.045	-0.145	40.00	109.3	32.60	19.10
03	1.010	-0.361	0.000	80.80	141.3	28.70	1.010	-0.361	0.000	79.10	141.3	28.70
04	0.974	-0.281	0.000	0.000	71.70	6.000	0.977	-0.282	0.000	0.000	71.70	6.000
05	0.980	-0.239	0.000	0.000	11.40	2.400	0.982	-0.240	0.000	0.000	11.40	2.400
06	1.000	-0.404	0.000	-10.20	16.80	11.30	1.000	-0.400	0.000	4.600	16.80	11.30
07	0.977	-0.370	0.000	0.000	0.000	0.000	0.986	-0.372	0.000	0.000	0.000	0.000
08	1.000	-0.370	0.000	13.30	0.000	0.000	1.000	-0.372	0.000	8.200	0.000	0.000
09	0.955	-0.419	0.000	0.000	44.30	24.90	0.973	-0.420	0.000	0.000	44.30	24.90
10	0.951	-0.426	0.000	0.000	13.50	8.700	0.966	-0.426	0.000	0.000	13.50	8.700
11	0.969	-0.418	0.000	0.000	5.300	2.700	0.977	-0.417	0.000	0.000	5.300	2.700
12	0.993	-0.436	0.000	0.000	9.200	2.400	0.983	-0.428	0.000	0.000	9.200	2.400
13	1.000	-0.451	0.000	40.50	20.70	8.700	0.980	-0.436	0.000	0.000	20.70	8.700
14	0.945	-0.464	0.000	0.000	22.40	7.500	1.000	-0.482	0.000	34.80	22.40	7.500
Suma			424.5	237.3	390.0	122.3			424.3	235.8	389.0	122.3
Total power loss												
Active [MW]	35.532						Actiea [MW]	35.343				
Reactive [Mvar]	115.07						Reactive [Mvar]	113.59				

3.2. Continuous power flow in voltage stability analysis

This section presents the voltage stability analysis before and after a contingency. In addition, it is analyzed the response of the system after installing the synchronous static compensation.

Figure 5 presents the voltage stability analysis in bus 11 of the EPS. It may be seen the behavior of the bus in three scenarios: i) normal operation (yellow curve), ii) disconnection of lines L2 and L4 (blue curve) and iii) voltage stability analysis when reactive compensation is incorporated through a STATCOM (red curve). Figure 5 presents the behavior of bus 11 in normal operating conditions with $\lambda_{max} = 3.7$ (approximately). When the load increase occurs with $\lambda_{max} = 3.2$, the stability margin is reduced. This occurs because the EPS is stressed and its maximum power transfer capacity is reduced, as shown in points 2-4 of Figure 5. The yellow and blue metrics represent the PV curve in conditions before and after the contingency without synchronous static compensation. An additional detail shown by Figure 5 is that the capacity of keeping the system stable decreases when the contingency occurs. When STATCOM is used, the voltage level increases and it is able to transmit slightly more power, as can be seen in points 4-6 of Figure 5. Therefore, the load factor level does not vary significantly when synchronous compensation is used, however, the profile improves. Points 1, 3, 5 of Figure 5 represent the optimal operating levels of the system where it can be seen more clearly that the power transmission capacity increases if the system has STATCOM to provide reactive power in specific operating conditions.

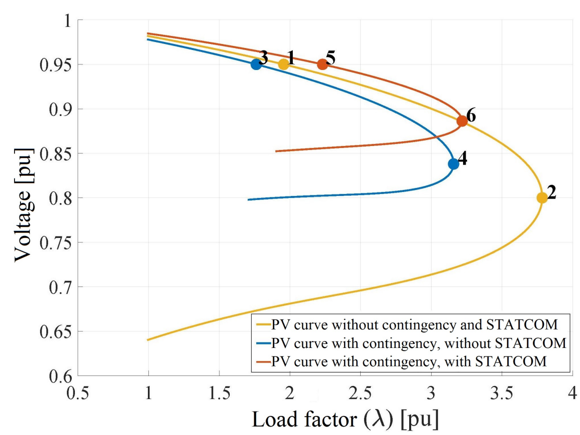

Figure 5. Voltage level as a function of the normal operating parameter, N – 1 contingency using reactive compensation

The Available Transmission Capacity (ATC) is calculated in Table 7. This analysis is carried out considering the worst contingency that may occur in the system; for this case, the worst contingency is when the line 2–4 is disconnected, TPlo represents the power demanded, i.e., the power required by the system for its normal operation. Pl are the losses present in the entire EPS, TTC is the maximum power value that may be present in the system, ETC represents the actual power in the EPS and TMR is the available power margin in which the electric system should remain before a voltage collapse occurs. Finally, it is proven that the STATCOM is capable of adjusting the voltage magnitudes in the buses of the EPS. A particular detail is that the STATCOM does not modify the active power values of the electric system. Based on the above, it may be inferred that the STATCOM adjusts the voltage levels injecting reactive power in the buses and maintains stable the voltage parameters under normal operating conditions, and increases the voltage in case of a fault so that the system remains stable.

Table 7. Available transfer capacity in the $N-1$ contingency

Bus N.°	Units	W/O STATCOM	With STATCOM
λ maximum	p.u	3.15760	3.21820
TPlo	MW	259.300	259.300
Pl	MW	15.2020	15.1810
TTC	MW	307.302	308.156
ETC	MW	259.300	259.300
TMR	MW	15.3651	15.4078
ATC	MW	32.6367	33.4477

The voltage stability analysis is performed with the metrics of Figure 6 considering different scenarios. The continuous power flow in initial conditions is computed with Figures 6(a, b and c), i.e., without contingencies and without the installation of synchronous static compensators. The voltage stability when a contingency is applied in lines L2 - L4 is analyzed in Figures 6(d, e and f). For the analysis mentioned it is proven the behavior of the PV curve for different values of λ. The PV curves shown in Figure 6 illustrate the magnitudes of the variables in the PQ buses. In the reference and generation buses, the voltage level is constant. From Figures 6(a-b) and 6(d-f) it may be inferred that as λ increases, the transmission capacity (resulting λ) decreases, and this occurs because the capacity of the electric transmission system operates inversely to the load, i.e., as the load increases the maximum electric power transfer capacity decreases. When a fault occurs (Figures 6(d-f) and the load factor increases, the voltage levels drop drastically putting the system in critical operating conditions, potentially leading it to experience a voltage collapse. An additional detail is that through the voltage stability analysis it is verified that, when a disconnection or fault occurs in the system, the voltage in all its PQ buses is reduced, mainly because they are load buses, but voltage drops are not significant in the generation buses.

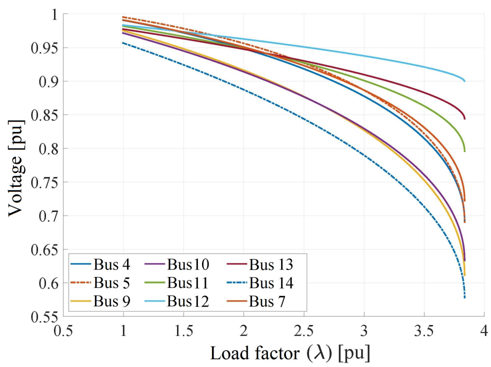

(a) Voltage with load factor ($\lambda = 1$)

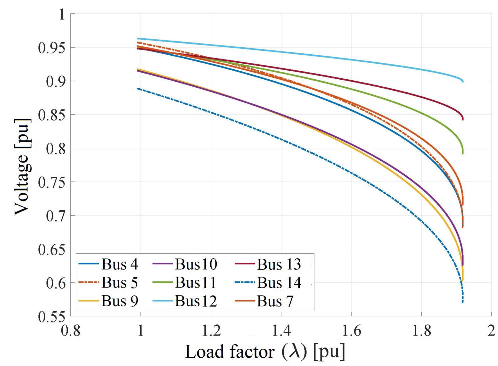

(b) Voltage with load factor ($\lambda = 2$)

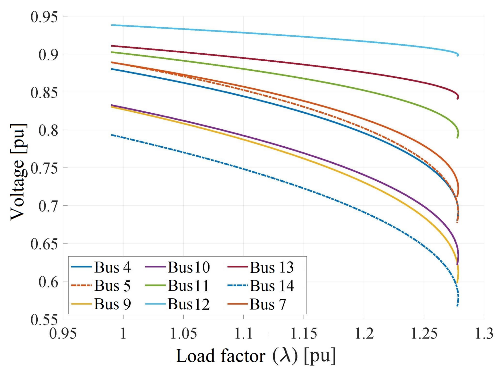

(c) Voltage with load factor ($\lambda = 3$)

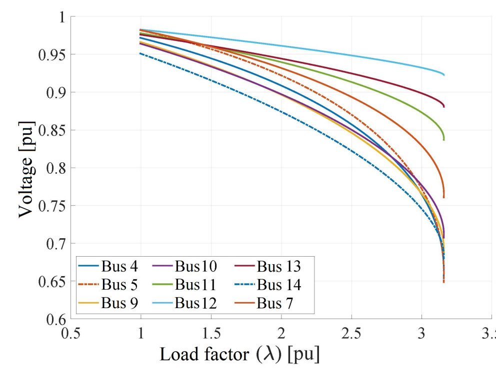

(d) Voltage with load factor ($\lambda = 1$)

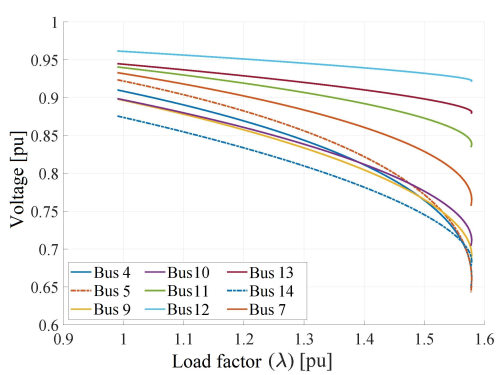

(e) Voltage with load factor ($\lambda = 2$)

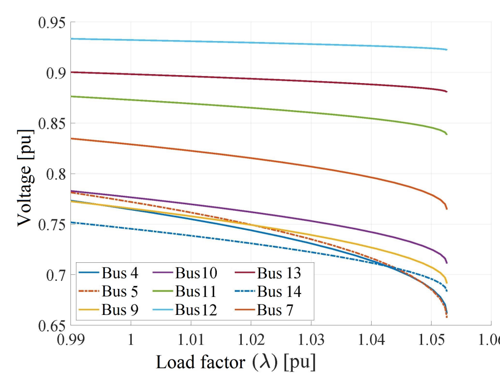

(f) Voltage with load factor ($\lambda = 3$)

Figure 6. PV curves with Continuous Power Flow (CPF) analysis. Figures a, b and c correspond to a CPF without STATCOM and without contingencies, and Figures d, e and f include a CPF without STSTCOM and a contingency produced by the opening of the 2-4 line

Figures 7 and 8 and Table 8 display the metrics for analyzing voltage stability and angular behavior in the buses considered; the voltage variable is analyzed with Figure 7; the angular variation analysis corresponds to Figure 8 together with Table 8. The PV curve that enables analyzing the voltage stability when line L2-L4 is disconnected is identified in Figure 7; this is considered the worst contingency of the electric system. In addition, it is seen the load factor variation reducing the stable operation margin of the electric system in the PQ buses when the load factor increases to $\lambda = 1.3$ pu. The voltage drop is seen in Figure 8. When a fault occurs, the voltage stability margin decreases, and this may be seen in Figure 7(b).

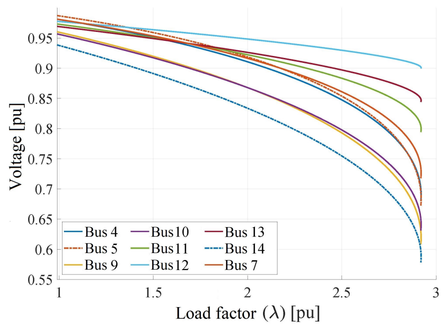

(a) Curva PV en condiciones normales

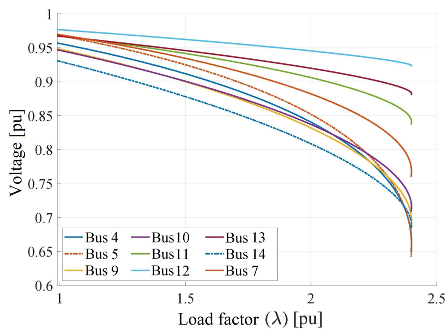

(b) Curva PV en contingencia $N-1$

Figure 7. PV curves in normal conditions and temporary opening of line 2-4, $\lambda = 1.3$, $t = 1$ s, $t = 1$ s

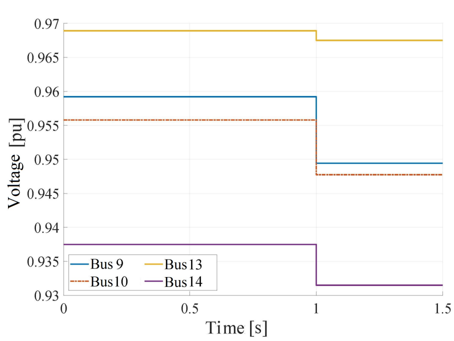

(a) Voltage profile

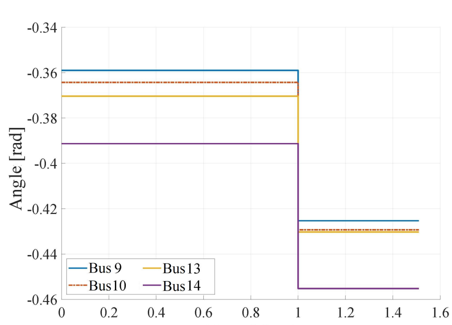

(b) Angle profile

Figure 8. Time domain curve in $N-1$ contingency in line 2-4

Table 8. Magnitudes of voltage and angle

Bus N.°	Normal conditions		Opening of line 2-4	
	Voltage	Angle	Voltage	Angle
01	1.060	0.000	1.060	0.000
02	1.045	-0.124	1.045	-0.115
03	1.010	-0.309	1.010	-0.346
04	0.980	-0.240	0.958	-0.310
05	0.985	-0.204	0.969	-0.252
06	1.000	-0.346	1.000	-0.405
07	0.981	-0.316	0.970	0.385
08	1.000	-0.317	1.000	-0.385
09	0.959	-0.358	0.949	-0.425
10	0.956	-0.364	0.948	-0.429
11	0.973	-0.358	0.969	-0.420
12	0.977	-0.368	0.977	-0.428
13	0.969	-0.370	0.968	-0.430
14	0.938	-0.391	0.932	-0.455

Figure 8(a) enables performing a wide analysis, because it shows an evaluation of the behavior of the buses in time domain when there is a 30% increment in the load, and the disconnection occurs in 1 second; the behavior of all buses is similar, therefore, Figure 8(a) will only present the buses in which there are significant variations due to the contingency generated. Therefore, when there is an unscheduled opening of any element of the electric system, mainly lines, this contingency affects all PQ buses since the supply of reactive power from the generation nodes to the loads is cut.

Figure 8(b) presents the behavior of the angle in time domain. The angular level varies according to the power flow and the initial conditions considered for the calculation; Figure 8(a) represents the angular variation in the PQ buses where there is a larger angular variability; it may be observed that the larger angular variation occurs in buses 9, 10, 13 and 14, where there is a drastic change in the voltage levels, as may be seen in Table 8. Consequently, it is concluded that the disconnection of an element of the system or a fault modify the system operating parameters and affect the maximum and minimum voltage operating limits.

Another very important aspect revealed by Table 8 is a summary of the voltage level variations and angular variation in each of the buses in time domain. Table 8 shows the voltage variations in all the buses; no changes are observed in the PV buses, but in the PQ buses the voltage varies due to the line disconnection. This occurs because the system power flow changes, due to the drastic topology change and the redirection of the power flow due to the opening of line $2-4$; an important point is that under operating conditions of 30% overload in the EPS, the voltage level in bus 14 is below 0.95 p.u.; a critical point of analysis is when the line is disconnected at bus 14 and its voltage magnitude is below 0.93 p.u.; i.e., the disconnection or fault in the system is affected by the connection to bus 14; a way to stabilize the parameters at such bus is through synchronous static compensation, which demonstrates that a candidate location to place the STATCOM is bus 14.

Table 8 enables analyzing the behavior of all system buses. The angular variation is different in all PQ buses and, unlike the voltage level, when an angular analysis is performed there is a variation in the PV buses; the only bus that remains under the same operating levels, both in voltage and angle, is the Slack bus, because when the power flow varies, the angle also varies. Consequently, Figure 8 shows the angular variation and Table 8 the voltage and angular variation in all system buses.

Figure 9 illustrates the voltage stability when a type II PSS controller is used, which implies that the possibility of analysis varies according to the PSS input signal (angular speed, voltage and power); when a speed controller is used, it is fundamental to assign various parameters for its full operation, namely, maximum and minimum voltage, stability gain. Figure 9 has a gain of 100 and it is seen that the generator controller starts to operate after line 2-4 is disconnected to maintain system stability. This type of control is known as primary voltage control, where the important issue is to stabilize voltage levels after the EPS experiences any contingency.

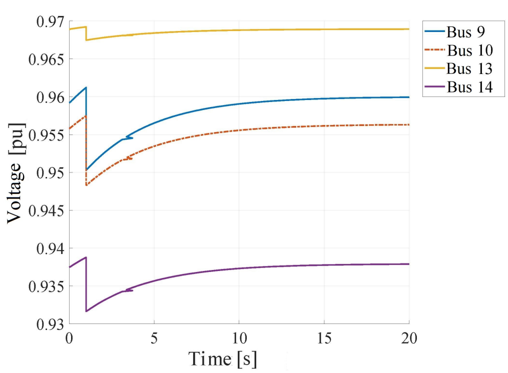

Figure 9. Voltage as a function of time in $N-1$ Contingency with the opening of line 2-4 with PSS voltage regulation

4. Conclusions

It has been possible to verify the reliability of the data obtained from the PSAT Toolbox and the performance, to provide results of voltage stability analysis and angular variation. Consequently, it is a reliable tool to perform detailed voltage stability analyses, considering the installation of STATCOM and PSS. The use of STATCOM FACTS devices has demonstrated to be an effective method to reduce the stress of the electric transmission network, and thus be able to maximize the power flow exchange from generation units to the different consumption points. In addition, the present research evidences that there are alternatives such as the PSS controllers to adjust the voltage in buses before deciding to install STATCOM, which has a higher cost.

On the other hand, the main contribution of this paper is considering a load factor that leads the EPS to operate in congestion conditions. Such congestion produces marginal operating costs, which raise the electric power transportation costs. In addition, contingencies are considered to be able to evaluate and select the most critical node (lowest voltage level), and thus be able to determine the location of reactive compensation. Therefore, this paper guarantees the optimal dimensioning of the STATCOM, to minimize power losses.

There is a big difference between the use of a FACTS compensator and the use of a PSS controller in the generator. FACTS is a device that improves stability of the voltage at the bus where it is located, and modifies voltage levels in most of the buses of the EPS seeking to maintain them at 1 pu. On the other hand, a PSS voltage control enables stabilizing the voltage levels in the generation buses through a control additional to the AVR. The gain is one of the fundamental variables to model PSS in the PSAT. The PSS gain is directly proportional to the voltage magnitude increase in the desired bus.

Therefore, PSS only actuates when there is a voltage drop in the buses of the generation units, thus maintaining a stable voltage in adjacent buses through electromechanical control of generation units. In addition, the paper proposes a methodology to guarantee voltage stability in the buses of the EPS using a STATCOM and a PSS controller, considering scenarios of $N-1$ contingency and load increase in the system. Finally, continuous power flows have been a fundamental tool to foresee the maximum voltage stability margin in an EPS.

References

[1] V. S. Rao and R. S. Rao, "Optimal Placement of STATCOM using Two Stage Algorithm for Enhancing Power System Static Security," *Energy Procedia*, vol. 117, pp. 575–582, 2017. [Online]. Available: http://dx.doi.org/10.1016/j.egypro.2017.05.151

[2] O. Samuelsson, S. Lindahl, P. Kundur, J. Paserba, V. Vittal, and T. T. Force, "Definition and Classification of Power System Stability," *Ieee Transactions on Power Delivery*, vol. 21, no. 1, pp. 446–447, 2006. [Online]. Available: https://doi.org/10.1109/TPWRS.2005.861952

[3] R. K. Varma and R. Salehi, "SSR Mitigation with a New Control of PV Solar Farm as STATCOM (PV-STATCOM)," *IEEE Transactions on Sustainable Energy*, vol. 8, no. 4, pp. 1473–1483, 2017. [Online]. Available: https://doi.org/10.1109/TSTE.2017.2691279

[4] A. K. Dwivedi and S. Vadhera, "Reactive Power Sustainability and Voltage Stability with Different FACTS Devices Using PSAT," in *2019 6th International Conference on Signal Processing and Integrated Networks, SPIN 2019*. IEEE, 2019, pp. 248–253. [Online]. Available: https://doi.org/10.1109/SPIN.2019.8711587

[5] B. Hernández, C. A. Cañizares, J. M. Ramírez, B. Hu, and M. Liu, "Secondary and tertiary voltage regulation controls based on regional optimal power flows," *20th Power Systems Computation Conference, PSCC 2018*, pp. 1–7, 2018. [Online]. Available: https://doi.org/10.23919/PSCC.2018.8442443

[6] J. Kumar and N. Kumar, "Determination and allocation of optimal size of TCSC and STATCOM for obstruction alleviation in power system," in *2018 2nd IEEE International Conference on Power Electronics, Intelligent Control and Energy Systems (ICPEICES)*, 2018, pp. 65–72. [Online]. Available: https://doi.org/10.1109/ICPEICES.2018.8897336

[7] L. Chun, J. Qirong, X. Xiaorong, and W. Zhonghong, "Rule-based control for statcom to increase power system stability," in *POWERCON '98. 1998 International Conference on Power System Technology. Proceedings (Cat. No.98EX151)*, vol. 1, 1998, pp. 372–376 vol.1. [Online]. Available: https://doi.org/10.1109/ICPST.1998.728989

[8] P. M. Chavan and G. P. Chavan, "Interfacing of hybrid power system to grid using STATCOM amp; power quality improvement," in *2017 International Conference on Information, Communication, Instrumentation and Control (ICICIC)*, 2017, pp. 1–5. [Online]. Available: https://doi.org/10.1109/ICOMICON.2017.8279079

[9] N. Mithulananthan, C. A. Cañizares, J. Reeve, and G. J. Rogers, "Comparison of PSS, SVC, and STATCOM controllers for damping power system oscillations," *IEEE Transactions on Power Systems*, vol. 18, no. 2, pp. 786–792, 2003. [Online]. Available: https://doi.org/10.1109/TPWRS.2003.811181

[10] C. Cañizares, T. Fernandes, E. Geraldi, L. Gerin-Lajoie, M. Gibbard, I. Hiskens Tf Past Chair, J. Kersulis, R. Kuiava, L. Lima, F. Demarco, N. Martins, B. C. Pal, A. Piardi, R. Ramos Tf Chair, J. Dos Santos, D. Silva, A. K. Singh, B. Tamimi, and D. Vowles, "Benchmark Models for the Analysis and Control of Small-Signal Oscillatory Dynamics in Power Systems," *IEEE Transactions on Power Systems*, vol. 32, no. 1, pp. 715–722, 2017. [Online]. Available: https://doi.org/10.1109/TPWRS.2016.2561263

[11] R. K. Varma and H. Maleki, "PV Solar System Control as STATCOM (PV-STATCOM) for Power Oscillation Damping," *IEEE Transactions on Sustainable Energy*, vol. 10, no. 4, pp. 1793–1803, 2019. [Online]. Available: https://doi.org/10.1109/TSTE.2018.2871074

[12] C. C. A. Gomes-Exposito, A. Conejo, "Electric Energy Systems Analysis and Operation," *Engineering - Technology*, p. 748, 2018. [Online]. Available: https://doi.org/10.1201/9781315192246

[13] M. Ahmadinia and R. Ghazi, "Coordinated Control of STATCOM and ULTC to Reduce Capacity of STATCOM," *26th Iranian Conference on Electrical Engineering, ICEE 2018*, pp. 1062–1066, 2018. [Online]. Available: https://doi.org/10.1109/ICEE.2018.8472712

[14] Y. T. Jeon, G. Farivar, C. D. Townsend, J. H. Park, and J. Pou, "Capacitor Voltage Shaper for Cascaded H-Bridge StatCom," *2018 IEEE 4th Southern Power Electronics Conference, SPEC 2018*, 2019. [Online]. Available: https://doi.org/10.1109/SPEC.2018.8635915

[15] A. S. Tamboli and H. T. Jadhav, "Hybrid STATCOM for Reactive Power Compensation," *Proceedings of the 2018 International Conference on Current Trends towards Converging Technologies, ICCTCT 2018*, pp. 1–5, 2018. [Online]. Available: https://doi.org/10.1109/ICCTCT.2018.8550889

[16] C. Xing, X. Xi, S. Li, and X. He, "Analysis on the Control Strategy and Response Characteristics of Large Capacity STATCOM Device in DC Converter Station," *2018 International Conference on Power System Technology, POWERCON 2018 - Proceedings*, no. 201804270001168, pp. 2873–2879, 2019. [Online]. Available: https://doi.org/10.1109/POWERCON.2018.8602013

[17] M. R. Wara and A. H. Rahim, "Supercapacitor E-STATCOM for power system performance enhancement," *1st International Conference on Robotics, Electrical and Signal Processing Techniques, ICREST 2019*, pp. 69–73, 2019. [Online]. Available: https://doi.org/10.1109/ICREST.2019.8644388

[18] J. Chen, P. Wang, Y. Hu, H. Shao, G. Li, X. Wang, and J. Qin, "Analysis of negative influence of harmonic circulation between parallel STATCOMs and suppression method," *PEDG 2019 - 2019 IEEE 10th International Symposium on Power Electronics for Distributed Generation Systems*, pp. 751–755, 2019. [Online]. Available: https://doi.org/10.1109/PEDG.2019.8807514

[19] H. A. Hassan, Z. H. Osman, and A. E.-A. Lasheen, "Sizing of STATCOM to Enhance Voltage Stability of Power Systems for Normal and Contingency Cases," *Smart Grid and Renewable Energy*, vol. 05, no. 01, pp. 8–18, 2014. [Online]. Available: https://doi.org/10.4236/sgre.2014.51002

[20] S. Isik, H. Nath, M. Alharbi, and S. Bhattacharya, "Negative Sequence Component Elimination with M-STATCOM for Versatile FACTS," *IECON Proceedings (Industrial Electronics Conference)*, vol. 2019-October, pp. 7069–7073, 2019. [Online]. Available: https://doi.org/10.1109/IECON.2019.8927805

[21] A. Raju, E. P. Cheriyan, and R. Ramchand, "Nearly Constant Switching Frequency Hysteresis Current Controller for Multilevel Inverter based STATCOM," *IEEE Region 10 Annual International Conference, Proceedings/TENCON*, vol. 2019-October, pp. 176–180, 2019. [Online]. Available: https://doi.org/10.1109/TENCON.2019.8929458

[22] V. Jain and N. Kumar, "Designing of Supplementary Controller for STATCOM for Damping of Oscillations in Power System," *Journal of The Institution of Engineers (India): Series B*, vol. 99, no. 5, pp. 419–429, 2018. [Online]. Available: https://doi.org/10.1007/s40031-018-0330-z

[23] G. G. Farivar, H. Dehghani Tafti, C. D. Townsend, and J. Pou, "Low Capacitance StatCom Capacitor Lifetime and Current Stress Analysis," *2019 9th International Conference on Power and Energy Systems, ICPES 2019*, no. 5, pp. 0–4, 2019. [Online]. Available: https://doi.org/10.1109/ICPES47639.2019.9105361

[24] A. M. Vural and K. C. Bayindir, "Optimization of parameter set for STATCOM control system," *2010 IEEE PES Transmission and Distribution Conference and Exposition: Smart Solutions for a Changing World*, pp. 1–6, 2010. [Online]. Available: https://doi.org/10.1109/TDC.2010.5484230

[25] A. B. Nassif and D. Fedaku, "A reactive power compensation scheme using distribution STATCOMs to manage voltage in rural distribution systems," *2020 IEEE Electric Power and Energy Conference, EPEC 2020*, vol. 3, pp. 1–5, 2020. [Online]. Available: https://doi.org/10.1109/EPEC48502.2020.9320005

[26] L. Sun, H. Zhang, Y. Cao, C. Li, Q. Guo, and Y. Zhu, "Design of micro dynamic simulation system for power system with wind power and VSC-HVDC," *2020 IEEE 4th Conference on Energy Internet and Energy System Integration: Connecting the Grids Towards a Low-Carbon High-Efficiency Energy System, EI2 2020*, no. 51627811, pp. 1355–1360, 2020. [Online]. Available: https://doi.org/10.1109/EI250167.2020.9347174

[27] S. Gurung, F. Jurado, S. Naetiladdanon, and A. Sangswang, "Comparative analysis of probabilistic and deterministic approach to tune the power system stabilizers using the directional bat algorithm to improve system small-signal stability," *Electric Power Systems Research*, vol. 181, no. June 2019, p. 106176, 2020. [Online]. Available: https://doi.org/10.1016/j.epsr.2019.106176

[28] W. Peres, I. C. Silva Júnior, and J. A. Passos Filho, "Gradient based hybrid metaheuristics for robust tuning of power system stabilizers," *International Journal of Electrical Power and Energy Systems*, vol. 95, pp. 47–72, 2018. [Online]. Available: http://dx.doi.org/10.1016/j.ijepes.2017.08.014

[29] H. Verdejo, V. Pino, W. Kliemann, C. Becker, and J. Delpiano, "Implementation of particle swarm optimization (PSO) algorithm for tuning of power system stabilizers in multimachine electric power systems," *Energies*, vol. 13, no. 8, 2020. [Online]. Available: https://doi.org/10.3390/en13082093

[30] T. Guesmi, A. Farah, H. H. Abdallah, and A. Ouali, "Robust design of multimachine power system stabilizers based on improved non-dominated sorting genetic algorithms," *Electrical Engineering*, vol. 100, no. 3, pp. 1351–1363, 2018. [Online]. Available: https://doi.org/10.1007/s00202-017-0589-0

[31] S. Orlando, "A Study of STATCOM on Stability and Efficiency in IEEE 14-bus," Master's thesis, 2016. [Online]. Available: https://bit.ly/3qT2McR